Journal of Macromolecular Science, Part A
Publication details, including instructions for authors and subscription information:
http://www.informaworld.com/smpp/title~content=t713597274

Multi-arm Star Polyisobutylenes. V. Characterization of Multi-arm Polyisobutylene Stars by Viscometry, Pour Points, Electron Microscopy, and Ultrasonic Shear Degradation

Timea M. Marsalkó[a]; István Majoros[a]; Joseph P. Kennedy[a]
[a] The Maurice Morton Institute of Polymer Science The University of Akron Akron, Ohio, USA

To cite this Article Marsalkó, Timea M. , Majoros, István and Kennedy, Joseph P.(1997) 'Multi-arm Star Polyisobutylenes. V. Characterization of Multi-arm Polyisobutylene Stars by Viscometry, Pour Points, Electron Microscopy, and Ultrasonic Shear Degradation', Journal of Macromolecular Science, Part A, 34: 5, 775 — 792
To link to this Article: DOI: 10.1080/10601329708014330
URL: http://dx.doi.org/10.1080/10601329708014330

J.M.S.—PURE APPL. CHEM., A34(5), pp. 775–792 (1997)

MULTI-ARM STAR POLYISOBUTYLENES. V. CHARACTERIZATION OF MULTI-ARM POLYISOBUTYLENE STARS BY VISCOMETRY, POUR POINTS, ELECTRON MICROSCOPY, AND ULTRASONIC SHEAR DEGRADATION†

TIMEA M. MARSALKÓ, ISTVÁN MAJOROS, and
JOSEPH P. KENNEDY*

The Maurice Morton Institute of Polymer Science
The University of Akron
Akron, Ohio 44325-3909, USA

ABSTRACT

Structure/property relationship of multi-arm star polyisobutylenes [*-(PIB)$_n$s] were characterized by a variety of techniques, including viscometry, pour points, electron microscopy, and ultrasonic degradation. The intrinsic viscosity of *-(PIB)$_n$s changes very little with temperature in the 30 to 100°C range, whereas that of linear PIBs of the same molecular weight increases strongly with temperature. Kinematic viscosity measurements of select *-(PIB)$_n$s gave viscosity indices in excess of 130. The viscosity of *-(PIB)$_n$s is mainly determined by the molecular weight of the arms and much less by the number of arms or overall molecular weights. Electron microscopy of *-(PIB)$_n$s indicates a compact spherical morphology, a conclusion that was substantiated by radius of gyration measurements. Pour points of *-(PIB)$_n$s are ~ -27°C. Ultrasonic studies gave insight into the mechanism of shear degradation of *-(PIB)$_n$s. These characteristics render *-(PIB)$_n$s of interest as rheology control additives for motor oils.

†For Paper IV, see N. Omura, A. Lubnin, and J. P. Kennedy, *Am. Chem. Soc. Symp. Ser.*, In Press.

INTRODUCTION

Star polymers are of great current theoretical and practical interest, and a variety of applicational possibilities are under intensive investigation [1–19]. Thus, stars of hydrogenated polyisoprene arms emanating from a polydivinylbenzene (PDVB) core are used as rheology modifiers in motor oils [19]. Stars with polymethacrylate (PMA) arms are studied for elastomer reinforcement [20]. The number of arms is important for enhancing performance of elastic networks: for example, a nine-arm star-block polymer produced an elastically effective network while networks of linear and four-arm block copolymers have disintegrated [21]. Star-blocks with polystyrene-*block*-polybutadiene (PSt-*block*-PBd) arms exhibit improved mechanical properties and processability over those of linear PSt-*block*-PBd-*block*-PSt analogues [1]. High polystyrene content (~25%) star-blocks offer rigidity, transparency, and good impact strength necessary for reinforcing and packaging applications (K-resins by Phillips) [22]. High polybutadiene (PBd) content star block copolymers have been used in hot melt and pressure-sensitive adhesives [23]. Exxon's "star-branched butyls," although the name implies star structures are, in fact, graft polymers having a short backbone (molecular weight of several thousand) which carry multiple high molecular weight butyl rubber arms (molecular weights in the range of millions). They offer a desirable balance of viscoelastic properties and show significantly improved processability [2–5].

Multi-arms star polyisobutylenes *-(PIB)$_n$s are also of great potential practical interest. The synthesis and molecular characterization of a large variety of *-(PIB)$_n$s have been described [24–32]. This paper concerns characterization of *-(PIB)$_n$s by various rheological investigations (i.e., dilute solution viscometry, kinematic viscosity and viscosity index studies, pour point measurements), sonic degradation studies, and electron microscopy.

EXPERIMENTAL

Materials

Acetone, hexanes, and tetrahydrofuran (Fisher Scientific Co.) were used as received. Tetrahydrofuran for size exclusion chromatography (SEC) was refluxed over calcium hydride. Mica and toluene (Aldrich Chemical Co.) were used as received. The commercial pour point depressant was received from BASF AG, Germany. The graphite electrode and platinum pellet were obtained from Accessories for Microscopy Co. Mineral Oil SN 200 (Sun Oil) and Reference Oil RL 34/02 (Petrolab Corp.) were used as received.

The syntheses of *-(PIB)$_n$s have been described [24–29]. The molecular parameters of the stars used in these investigations are:

Star 8-110: $\overline{M}_{w,\,Star}$ = 1,134,400 g/mol, $\overline{M}_{w,\,Arm}$ = 8,000 g/mol, $\overline{N}_{w,\,Arm}$ = 110

Star 28-30: $\overline{M}_{w,\,Star}$ = 907,100 g/mol, $\overline{M}_{w,\,Arm}$ = 28,100 g/mol, $\overline{N}_{w,\,Arm}$ = 30

Star 54-32: $\overline{M}_{w,\,Star}$ = 2,425,000 g/mol, $\overline{M}_{w,\,Arm}$ = 54,500 g/mol, $\overline{N}_{w,\,Arm}$ = 32

The two digit number of these stars indicates the weight-average molecular weight of the arms/1000 and the number of arms; for example Star 8-110 stands for a

star whose arm molecular weight is $\overline{M}_{w,\,Arm}$ = 8000 g/mol and having 110 arms ($\overline{N}_{w,\,Arm}$).

Instrumentation

A Schott Automated Viscometer (Model AVS 350) was operated with calibrated capillary viscometers immersed in a thermostated silicon oil bath controlled and maintained to ±0.2°C accuracy by a Fisher Isotemp Immersion Circulator (Model 730). Efflux times were measured by a laser-light-triggered integral watch and were collected by the VP 3.8 software of the manufacturer. Ubbelohde-type viscometers in the 0.1 to 10 cSt kinematic viscosity range were manufactured and calibrated by the Scott Co., and Cannon-Fenske viscometers in the 6 to 215 cSt kinematic viscosity range were manufactured and calibrated by the Cannon Instrument Co. The calibration constants were checked by using toluene or a mineral oil with a known kinematic viscosity.

Transmission electron micrography was carried out with a transmission electron microscope (Japan Electronic Optics Limited, Model 1200 EXII) operated at 100,000 V and equipped with a CCD Camera Control Unit (Gatan Co., Model 673-0200).

The ultrasound sonicator was by Sonic System, Inc. The sonicator plate was maintained at −15°C by conductive cooling using a recirculating bath (Neslab Model RTE-100LP) filled with a mixture of ethylene glycol/distilled water 50/50 v/v%.

The size exclusion chromatograph, SEC, was assembled from a Waters chromatography pump (Model 510), an ultraStyragel column set consisting of 100, 500, 1000, 10,000, and 100,000 Å columns maintained at 35°C as the stationary phase, a Waters 410 Differential Refractometer, a Waters 440 UV detector operated at 254 nm, and an on-line three-angle (45°, 90°, and 135°) laser-light-scattering (LLS) MiniDawn detector (Wyatt Technology Corporation) operating at 690 nm. THF was the mobile phase at a flow rate of 1 mL/min, and sulfur was the internal standard. PIB and PSt calibrations were obtained with narrow dispersity ($\overline{M}_w/\overline{M}_n$ < 1.1) PIB and PSt standards. RI and UV data were collected and analyzed with a Nelson-Analytical 2600 chromatography (SEC option) software. The LLS detector was calibrated to toluene at a flow rate of 1 mL/min, and the data were analyzed with Astrette 3.4 and Astra 4.0 for Windows software [24–30].

Procedures

Dilute solution viscometry was carried out with toluene. Unreacted PIB prearm contaminants in *-(PIB)$_n$ samples were removed by fractionation. Thus, to 5 g samples dissolved in 25 mL hexanes was slowly added under stirring ~15 mL acetone; the upper hexanes phase which contains the unlinked arms was separated from the lower hexanes/acetone phase which contains the stars. After evaporating the volatiles, the purity of the residue was analyzed by SEC.

For dilute solution viscometry the purified *-(PIB)$_n$ was dried and toluene solutions were prepared at five concentrations ranging from 0.5 to 5 g in 100 mL at 25°C. Efflux times were corrected by the "Hagenbach correction" [33]. Intrinsic

viscosities were obtained from intercepts of inherent viscosity vs concentration plots at 30, 37, 50, 70, 90, and 100°C.

Kinematic viscosities were determined according to ASTM D 445. One gram of polymer was dissolved in 100 mL Mineral Oil SN 200 at ~100°C under a N_2 atmosphere. Efflux times were measured at 40 and 100°C by a Cannon viscometer (Number G 172 A) and a stopwatch. Kinematic viscosities were obtained from the product of efflux time multiplied by the calibration constant of the viscometer.

The viscosity index (VI) was calculated from kinematic viscosities (ν) determined at 40 and 100°C in mineral oil according to ASTM D 2270-91 (*Method B* since the VI is above 100).

Pour points were determined according to ASTM D 97. Thus 1.5 grams of *-$(PIB)_n$ was dissolved in 100 mL Mineral Oil SN 200 at ~100°C under a N_2 atmosphere, and after a day of thermal relaxation at room temperature, the solution was poured into a large tube and placed into a bath at 0°C. After 30 minutes of thermostating, the solution was tilted from the vertical to the horizontal position for 10 seconds. The pour point was reached when the surface of the solution did not move. The procedure was repeated by decreasing the temperature in 3°C increments.

Electron micrographs were obtained on a clean mica surface covered with a layer of carbon by evaporating a graphite electrode under high vacuum for 20 minutes. Then a solution of *-$(PIB)_n$, 1×10^{-4} vol%, in toluene was sprayed in a single layer onto the graphite surface. The plate with the *-$(PIB)_n$ coating was dried and coated with platinum by evaporating platinum pellets from a 30° angle for 5 minutes in vacuum. The graphite-based film was carefully transferred from the mica to a microscopic copper grid, and the surface was studied at 200,000 magnification. The size of the image of the *-$(PIB)_n$ was estimated by the scale provided with the electron micrographs.

Sonic shear stability was determined according to ASTM D 445. In the test of a defined volume of oil is sonicated in a sonic oscillator for a certain time and the changes in viscosity are determined. Standard reference fluids of readily sheared or shear-resistant oils or polymers are run simultaneously to make sure that the equipment imparts a controlled amount of sonic energy to the sample. The power setting of the sonicating equipment was calibrated with a mineral oil standard (R 34/02) to achieve 20% loss of kinematic viscosity of the reference oil measured after 10 minutes sonication at 60 W setting at 100°C. During sonication the samples [1 g of *-$(PIB)_n$ or PIB dissolved in 100 mL Mineral Oil SN 200] were immersed in a cooling bath at −15°C. (Thirty milliliters of an oil sample in a 50-mL beaker was immersed into the cooling bath and was thermostated for 10 minutes.) The sonic horn was immersed 4 cm below the surface of the oil. The samples were sonicated for 5, 10, 20, and 40 minutes. Power and temperature values were recorded 1 minute after sonication started and 1 minute before sonication stopped. Between sonications the sonic horn was rinsed with hexanes, dried with a paper towel, and cooled to room temperature for 20 minutes. Kinematic viscosities (ν) were measured at 100°C. The viscosity loss (% V_{loss}) is expressed as

$$\% V_{loss} = \frac{\nu_{\text{before radiation}} - \nu_{\text{after radiation}}}{\nu_{\text{before radiation}}} \times 100$$

The effect of sonication, i.e., molecular weight loss, was further examined by SEC.

RESULTS AND DISCUSSION

Rheological Investigations

Purification of *-(PIB)$_n$s

Dilute solution viscometry requires well-defined monodisperse stars. Therefore, preparatory to dilute solution studies, monodisperse stars were obtained by removing unlinked PIB arms and higher-order stars [24–30] by hexane/acetone fractionation. Figure 1 shows RI-SEC eluograms of Star 54-32 before and after purification. The small peak (~33 minutes elution time) indicates ~10% unlinked PIB arm contaminants in the sample before purification. The purified star (top eluogram) was used for viscometry measurements.

Dilute Solution Viscometry: Intrinsic Viscosities, Branching Coefficients, and Radius of Gyration

High molecular weight star polymers exhibit much lower intrinsic viscosities than linear polymers of the same molecular weight and composition in a Θ solvent or a good solvent [1, 34–43]. Stars are relatively dense and compact because of the reduced mobility of the arms due to the core so that the expansion of the arms is restricted and the density of the arm segments close to the core increases [44–47]. In contrast, linear polymers are unrestricted and may assume relatively larger volumes. Intrinsic viscosities of star polymers have not been intensively investigated over a wide temperature range. While ample literature deals with dilute solution viscosity at room temperature in different solvents [1, 34–47], a very limited number of

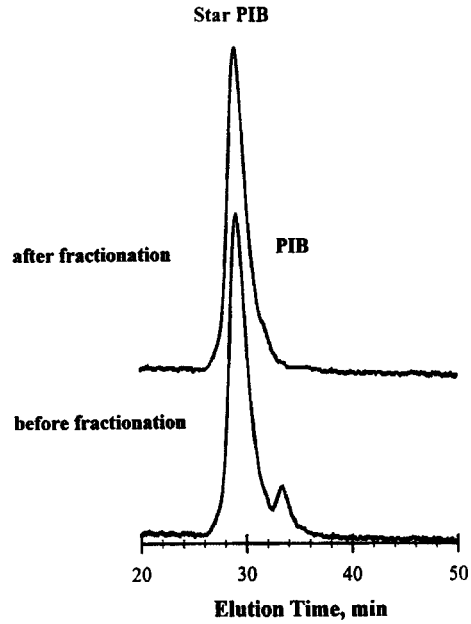

FIG. 1. RI-SEC eluograms of Star 54-32 before and after fractionation. ($\overline{M}_{w,\,Star}$ = 2,425,000 g/mol, $\overline{N}_{w,\,Arm}$ = 32, $\overline{M}_{w,\,Arm}$ = 54,500 g/mol; for synthesis condition see Ref. 27.)

publications concern temperature-dependent dilute solution viscosities of star polymers [40, 44, 46].

Dilute solution viscosities of select and fractionated *-(PIB)$_n$s and PIB arms were studied by using toluene solutions over the 30 to 100°C range. The needed K and a Mark–Houwink constants over the 30 to 100°C range are available for polyisobutylene in toluene only [48].

Figure 2 shows efflux time vs temperature plots of three representative stars. The efflux times of Star 8-110 are only slightly higher than those of toluene and much lower than those of Star 28-30 and Star 54-32. The efflux times of toluene decrease with increasing temperature, and the same tendency is observed for the solutions of the stars. The efflux time vs temperature curves are similar at other concentrations (c = 0.0025, 0.005, 0.0075, and 0.0125 g/mL toluene) as well (not shown).

Figure 3 illustrates intrinsic viscosities at six temperatures of Star 54-32, the PIB arm of $\overline{M}_w$ = 54,500 g/mol, and linear PIB of $\overline{M}_w$ = 116,100 g/mol, (i.e., a "two-arm" star), and a linear PIB of $\overline{M}_w$ = 2,425,000 g/mol (i.e., the $\overline{M}_w$ of Star 54-32). Its intrinsic viscosity was calculated by $[\eta] = KM^a$. The intrinsic viscosities, $[\eta]$s, of stars ($[\eta]_{Star}$) are very low relative to those of linear PIBs ($[\eta]_{Linear}$) at the same molecular weight, and close to those of the two-arm star or the PIB arm. Evidently the $[\eta]_{Star}$ is mainly determined by the individual prearm molecular weight and not by the overall $\overline{M}_{w,\,Star}$. The $[\eta]_{Star}$ and the $[\eta]_{Linear}$ of the arm slightly increase with temperature. However, the temperature response of the high molecular weight linear PIB is much stronger, i.e., $[\eta]_{Linear}$ increases very strongly over the temperature range investigated.

The difference in the behavior of the *-(PIB)$_n$ and the linear PIB of the same molecular weights is due to their fundamentally different architectures: The hydrodynamic volume of the linear PIB is much larger than that of the star since the mobility of the linear chain is not restricted. In contrast, the hydrodynamic volume of stars reflects those of the arms and therefore leads to smaller $[\eta]$. The

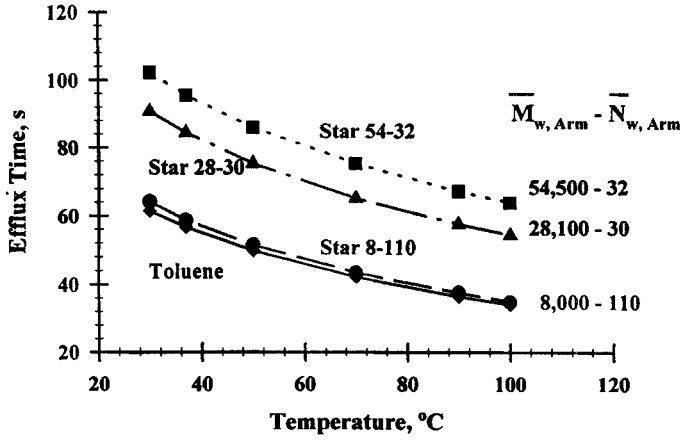

FIG. 2. Efflux time as a function of temperature for toluene, Star 8-110, Star 28-30, and Star 54-32 (c = 0.01 g/mol).

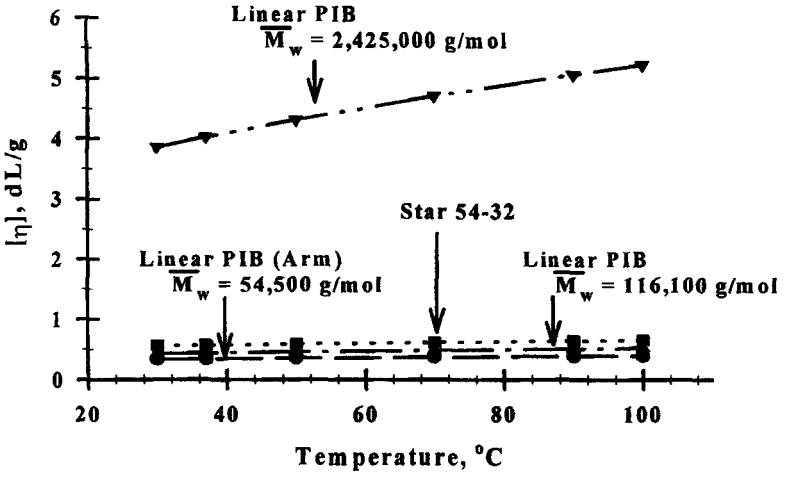

FIG. 3. Intrinsic viscosity as a function of temperature for Star 54-32, linear PIB of $\overline{M}_w$ = 54,500 g/mol (arm), and 116,100 g/mol ("two-arm" star of Star 54-32).

smaller hydrodynamic volume of the star is due to restricted mobility caused by the core.

The intrinsic viscosity of the linear PIB of $\overline{M}_w$ = 116,100 g/mol (i.e., of the "two-arm" star) is somewhat smaller than that of the multi-arm Star 54-32. This may be because the volume of a star is not only the sum of the hydrodynamic volumes of the arms but the core may also contribute. The hydrodynamic volume of a star also increases because the arms in the vicinity of the core are forced to assume extended conformations due to steric restrictions.

Figure 4 summarizes the $[\eta]$s of three *-(PIB)$_n$s together with three corresponding linear PIBs of the same molecular weights over the 30 to 100°C temperature range. Similar to the results shown in Fig. 3, the $[\eta]_{Star}$s are much lower than those of the $[\eta]_{Linear}$s, and the temperature changes of $[\eta]_{Star}$s are insignificant relative to those of the $[\eta]_{Linear}$s. The temperature response of Star 8-110 is almost zero. Evidently the large number of short arms are already fully extended at 30°C and there is very little if any conformational change with increasing temperature. The expansion of the largely crosslinked core is neglected in this model.

Figure 5 illustrates branching coefficients $\left(\text{i.e., } g^* = \left|\frac{[\eta]_{Star}}{[\eta]_{Linear}}\right|^{T,M}_{solvent}\right)$ as a function of temperature. All the g^*s are very small, less than 0.2, and decrease only slightly with increasing temperature. Apparently the overall trends are unaffected by the number of arms and the molecular weights of the arms. The explanation for the small g^* values and their inverse temperature responses resides in the definition: $[\eta]_{Star}$ is small and it increases only slightly with temperature (see Fig. 3), and this quantity is divided by $[\eta]_{Linear}$ which is about five times larger and whose temperature dependence is much larger than that of the $[\eta]_{Star}$. Interestingly, the g^*s of Star 8-110 are distinctly lower than those of Stars 28-30 and 54-32. The explanation for this may also come from the definition of g^*: $[\eta]_{Star}$ is governed by arm molecular weights so that g^* will be small when the arms are short; $[\eta]_{Linear}$ (calculated by the

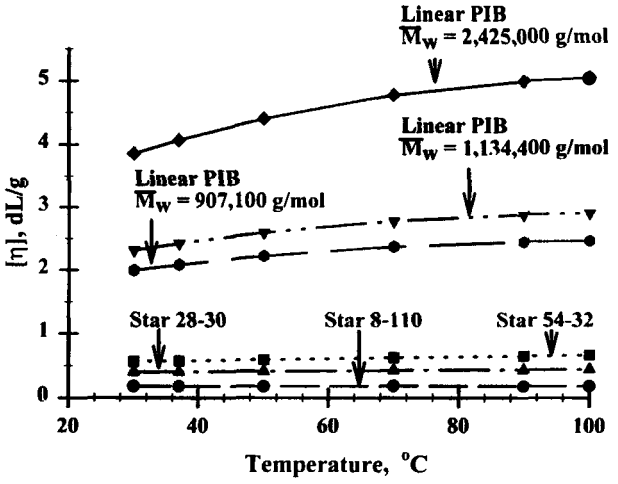

FIG. 4. Intrinsic viscosity as a function of temperature for Star 28-30 and the corresponding linear PIB of $\overline{M}_w$ = 907,100 g/mol; Star 8-110 and the corresponding linear PIB of $\overline{M}_w$ = 1,134,400 g/mol; and Star 54-32 and the corresponding linear PIB of $\overline{M}_w$ = 2,425,000 g/mol.

use of $[\eta] = KM^a$, where $M = \overline{M}_{w,\,Star}$, which is approximately equal to $\overline{N}_{w,\,Arm} \times \overline{M}_{w,\,Arm}$ plus the weight of the core per star) will be very large when $\overline{N}_{w,\,Arm}$ is large (i.e., 110); therefore g^* will be very small for a star with many short arms. We expect g^* of Star 8-30 to be much higher than that of Star 28-30.

A variety of methods based on various theories have been proposed to calculate g^* from $[\eta]$. Table 1 displays g^*s calculated by Stockmayer and Fixman (S&F) [49], Zimm and Kilb (Z&K) [50], Random Walk (R.W.) [51], by a general calculation for small and large number of arms (SNA and LNA, respectively) [52], and by Fetters [53]. Fetters's empirical equation was derived for polyisoprene and polysty-

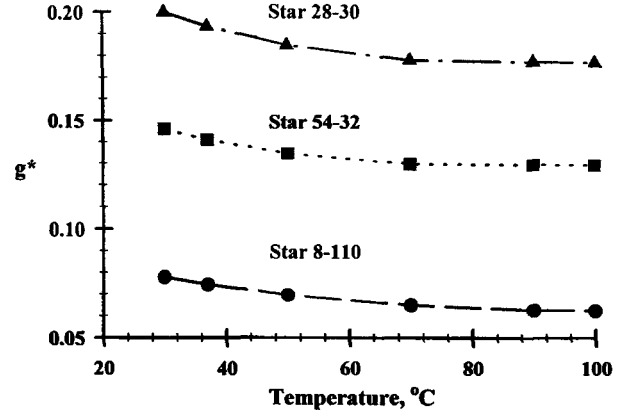

FIG. 5. g^* as a function of temperature for Star 8-110, Star 28-30, and Star 54-32.

TABLE 1. Experimental and Predicted g^*s

Star	$g^*_{30°C}$, Experimental	S&F	Z&K	R.W.	SNA	LNA	Fetters
8-110	0.078	0.012	0.178	0.027	0.027	0.032	0.05
28-30	0.200	0.074	0.338	0.097	0.100	0.118	0.16
54-32	0.185	0.068	0.328	0.092	0.094	0.110	0.15

rene stars dissolved in good solvents. Evidently, the g^*s calculated by Fetters's empirical equation come closest to the measured values.

Figure 6 summarizes radii of gyration (R_g) calculated from experimental $[\eta]_{Star}$ data for Start 54-32 as a function of temperature. Two sets of calculations were performed: a) assuming random coil conformation [54] and b) assuming rigid sphere conformation [55]. Obviously neither assumption can be strictly valid for stars whose conformation must be somewhere between these two limits. In general we visualize stars as assuming conformations somewhere between the rigid sphere and random coil limits: the rigid sphere conformation is proposed to prevail in the vicinity of the core, whereas the random coil conformation will preferentially exist toward the ends of reasonably long arms removed from the steric restriction imposed by the core. And we propose a gradual transition exists between these limits as one moves from the core toward the ends of the corona. Interestingly, the experimental R_g (obtained by LLS) at 35°C for Star 54-32 is $\sim 27 \pm 2$ nm (see Fig. 6), a value which is quite close to that calculated by assuming the rigid sphere limit. According to this evidence, the microstructure of Star 54-32 is much closer to the rigid sphere than to the random coil.

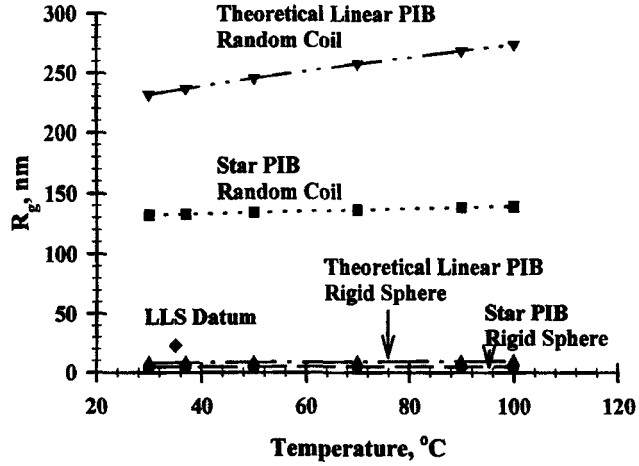

FIG. 6. Calculated radii of gyration of Star 54-32 and linear PIBs assuming the random coil and rigid sphere model as a function of temperature. The LLS datum indicates the experimentally found radius of gyration of Star 54-32 at 35°C.

Viscosity Index

The viscosity index (VI) is a commonly used measure of the viscosity change of a fluid with temperature [56, 57]. The higher the VI, the smaller the relative change in viscosity with temperature. The VI is calculated from kinematic viscosities measured at 40 and 100°C [57]. The VI cannot be calculated for an oil with a kinematic viscosity of less than 2.0 mm^2/s. The VI is reported to the nearest whole number. A motor oil should have a relatively low viscosity at low temperatures (for efficient starting and pumping characteristics) and a high one at elevated temperatures to maintain satisfactory lubrication. Common multigrade motor oils have VIs in the 130 to 170 range.

The VIs of oil solution of Star 28-30 and Star 54-32 were determined according to ASTM D 2270. Table 2 shows kinematic viscosities measured at 40 and 100°C, and the VIs calculated from these measurements. Thus the VI of *-$(PIB)_n$s are certainly in the technologically desired range. However, further optimization studies would be needed to enhance the VIs of blends modified with *-$(PIB)_n$. The difference in the VIs between the two stars suggests that the VI is moderately sensitive to the $\overline{M}_{w,\,Arm}$.

Pour Point

The pour point is one of several methods that characterizes the fluidity of an oil and is an index of the lowest temperature of its utility for lubrication applications [58]. Above the pour point the oil is a viscous liquid which can provide lubrication without inhibiting the movement of rotating parts. The pour point is determined by first heating the blend to ~100°C, cooling it at a specified rate, and examining its flow at 3°C intervals. The lowest temperature at which the oil is still fluid is the pour point.

Table 3 summarizes pour points determined according to ASTM D - 97 of Star 28-30, Star 54-32, linear PIB of $\overline{M}_w$ = 116,100 g/mol, and Shell Chemical Company's Shellvis SV 250 (hydrogenated polyisoprene star polymer) dissolved in Mineral Oil SN 200.

The pour points of linear PIB and *-$(PIB)_n$s are similar to Shellvis SV 250. In contrast to earlier reports which provide evidence that linear PIB has a negative impact on pour point [59], *-$(PIB)_n$s decreased the pour point of the base oil: The

TABLE 2. Kinematic Viscosities and Viscosity Indices

	Kinematic viscosity, mm^2/s		
Name	40°C	100°C	VI
Mineral Oil SN 200	44.5	6.6	99
Star 28-30[a]	66.0	9.7	130
Star 54-32[a]	76.6	11.2	137

[a]1 wt% in Mineral Oil SN 200.

TABLE 3. Pour Points

Name	T, °C
Mineral Oil SN 200	−15
Star 28-30[a]	−27
Star 54-32[a]	−27
Linear PIB,[a] $\overline{M}_w$ = 116,100 g/mol	−27
Shellvis SV 250[a]	−24

[a]1.5 wt% in Mineral Oil SN 200.

pour point of Mineral Oil SN 200 is −15°C, whereas those of the *-(PIB)$_n$s and the linear PIB are −27°C. Commercial pour point depressants are usually blended into motor oils; therefore, pour points of stars in the oil blends are expected to be below −27°C.

Transmission Electron Microscopy of a Select *-(PIB)$_n$

Transmission electron microscopy of star polymers has usually been restricted to studies concerning compositional inhomogeneities [1, 60]. An electron micrograph of a star PBd-*block*-PSt emanating from a PDVB core shows a lamellar array of PSt domains [1]. The contribution of the PDVB core to the morphology of these systems remains to be clarified. Two distinct polymer phases and a random arrangement of PSt domains irrespective of composition were observed. Electron microscopy of star-block copolymers with at least eight arms showed a "double-diamond" morphology beyond a certain block molecular weight [60, 61]. Two-phase morphology was also observed for rigid-rod star-block copolymers having a different number of arms. Changes in the number of arms did not affect the phase transition [60]. Images of individual star polymers have not yet been obtained.

An electron micrograph of Star 54-32 was obtained to characterize the shape of an individual star molecule. After very careful sample preparation (dust-free conditions), Pt-stained images were studied by transmission electron microscopy. Figure 7 shows an image of the star. The micrograph reveals a spherical object with a white shadow in the center. The image suggests a spherical shape for the star, although it may be influenced by sample preparation conditions, i.e., type of solvent used and rate of solvent evaporation. The diameter of the sphere is 55 ± 4 nm which is in satisfactory agreement with R_g = 27 ± 2 nm obtained by LLS (see above). These studies were difficult to perform because the PIB chain tends to degrade and evaporate under sustained high energy electron beams [62].

Sonic Shear Stability

The Orbahn method [63] and the Engine Test [64] are standard industrial methods to determine the mechanical shear stability of oil additives. However, these methods require relatively large amounts of samples (300 to 1000 g) and expensive specialized instrumentation. In contrast, sonic testing by the use of relatively inexpensive ultrasound horns requires only 0.5–1.0 g polymer and provides some infor-

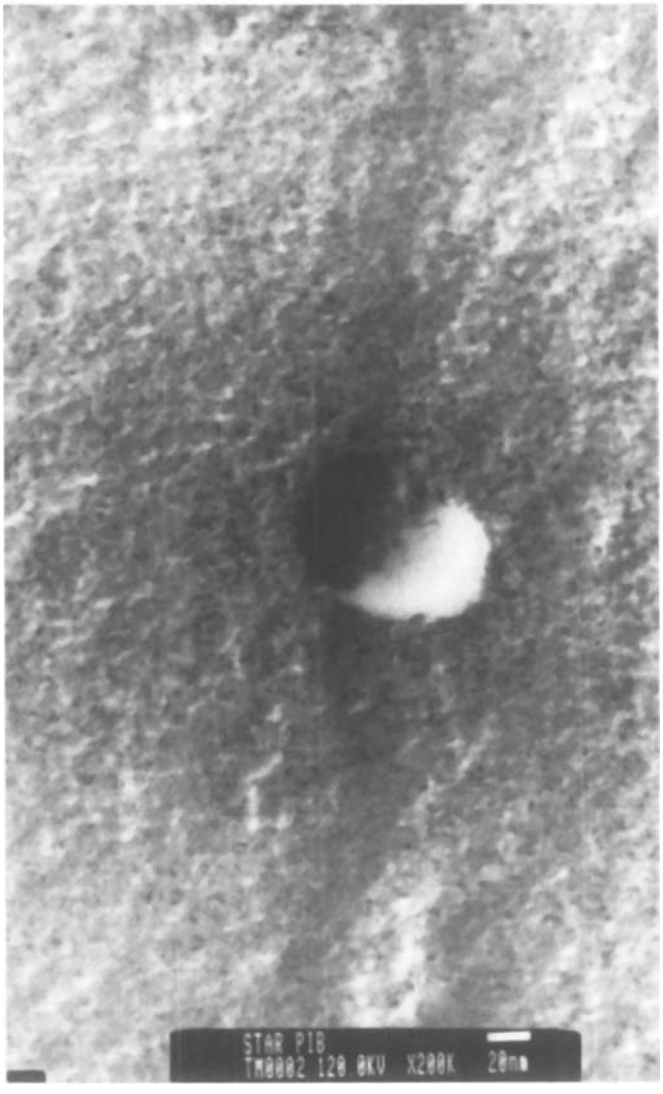

FIG. 7. Electron microscopic image of platinum-stained Star 54-32.

mation in regard to mechanical shear stability [65–67]. The shear stability of an oil which contains polymeric additives is determined in terms of permanent viscosity loss upon sonication in the absence of thermal and oxidative influences [68]. The correlation between mechanical and sonic shear degradation, however, has not yet been worked out precisely [65, 66].

The sonic shear stabilities of Star 28-30 and Star 54-32 together with a linear PIB of $\overline{M}_w$ = 116,100 g/mol (a two-arm model of Star 54-32) were investigated. These stars have approximately the same number of arms (i.e., $\overline{N}_{w,\,Arm}$ = 30 and 32) but different arm molecular weights (i.e., $\overline{M}_{w,\,Arm}$ = 28,100 and 54,500 g/mol). Figures 8 and 9 show kinematic viscosities and the retention of kinematic viscosity

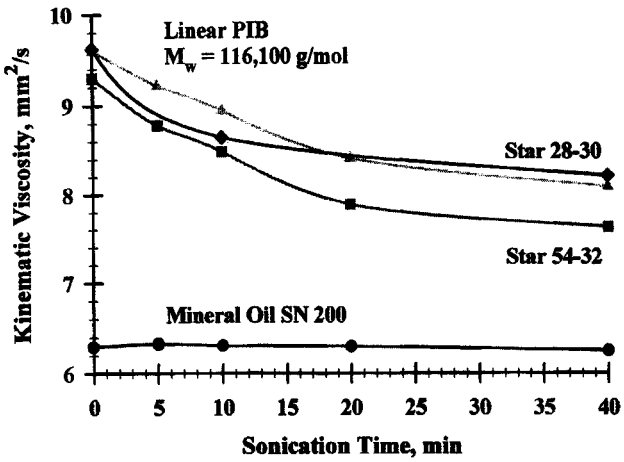

FIG. 8. Kinematic viscosities of Star 28-30, Star 54-32, linear PIB (all in 1 wt% solutions of Mineral Oil SN 200), and Mineral Oil SN 200 at 100°C as a function of sonication time.

(%), respectively, as a function of time of the starting and sonicated oil samples containing *-$(PIB)_n$s. Sonication for 40 minutes reduces the kinematic viscosity of Mineral Oil SN 200 insignificantly (~3%) whereas those of the linear PIB, Star 54-32, and Star 28-30 were reduced noticeably, i.e., from 9.87, 9.3, and 9.62 mm^2/s to 8.1 (18% loss), 7.63 (18% loss), and 8.21 (15% loss) mm^2/s, respectively. The kinematic viscosities of stars and PIB were similar during shorter sonication (5 and 10 minutes). According to the results shown in Fig. 9, the viscosity loss of Star 28-30 seems to level off after 20 minutes of sonication (~12% viscosity loss), whereas Star 54-32 and the linear PIB continue to degrade.

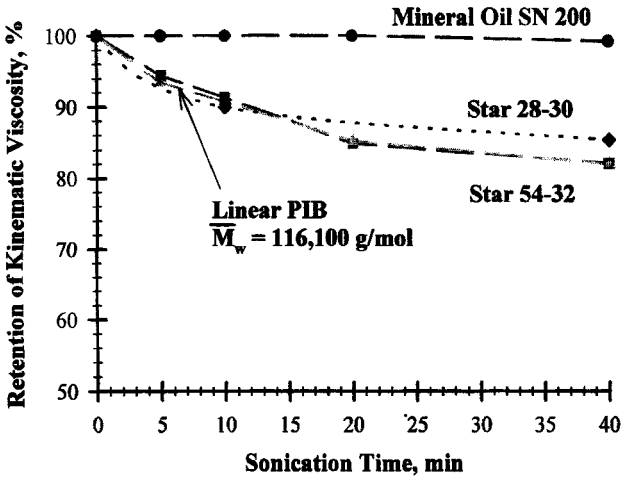

FIG. 9. Retention of kinematic viscosities of Star 28-30, Star 54-32, linear PIB, and Mineral Oil SN 200 at 100°C as a function of sonication time.

Efforts were made to understand the details of sonic degradation. Thus small amounts of sonicated samples were analyzed by SEC measurements. Figure 10 shows the SEC-RI traces of the two *-$(PIB)_n$s and the linear PIB at different sonication times. Unsonicated Star 54-32 contains two major components: *-$(PIB)_n$ (which elutes at ~29 minutes) and unlinked PIB arm (which appears at ~33.5 minutes). The star exhibits a tail in the high molecular weight region (lower elution time), most likely due to higher order stars. After 5–10 minutes of sonication the high molecular weight tail is strongly diminished, after 20 minutes the peak associated with the *-$(PIB)_n$ is largely decreased, and after 40 minutes of sonication only a small amount of *-$(PIB)_n$ (peak at ~31.5 minutes) remains. The amount of unlinked PIB arms increases strongly after the first 10 minutes of sonication while the amount of higher order stars diminishes. Surprisingly, the shape and position of the peak associated with the unlinked PIB arms do not change upon sonication, which suggests that the arms break off close to the core, i.e., where steric hindrance is largest. After exhaustive sonication (40 minutes) the amount of PIB arm increases and arm degradation also proceeds, as indicated by the broadening of the peak at ~33.5 minutes and by the appearance of a low molecular tail (at ~34 minutes).

Two chromatograms of Star 28-30 were also obtained (see Fig. 10). The virgin sample contained two components: the *-$(PIB)_n$ (peak at ~30 minutes), and the unlinked PIB arms (at ~35 minutes). After 40 minutes of sonication these two components were still present, although the amount of unlinked PIB arms had increased and the primary star had lost its high molecular weight tail. Interestingly, the unlinked PIB arms did not degrade. This is a striking difference as compared with Star 54-32: In the case of Star 28-30 the higher order stars had disappeared (no tail at higher molecular weights) but the primary star survived sonication. The fact that the amount of unlinked PIB (peak at ~35 minutes) increases with sonication time leads to the same conclusion as derived above: Higher order stars are more

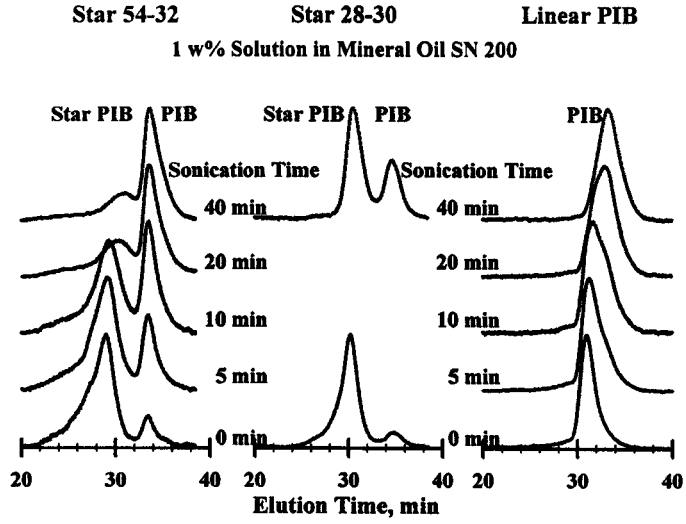

FIG. 10. RI-SEC eluograms of Star 54-32, Star 28-30, and linear PIB of $\bar{M}_w$ = 116,100 g/mol before and after sonication.

susceptible to sonication and they readily break apart to produce unlinked PIB arms and cores. The cores are most likely removed by filtration during work-up. The large increase in the amount of PIB also indirectly proves the existence of higher order stars: The overall amount of higher order stars that have disappeared is much lower than the overall amount of linear PIB that has formed. It is difficult to express this finding more quantitatively because calculations would demand peak deconvolution and knowledge of refractive indexes.

In respect to sonic degradation, the molecular weight of the arms is evidently of great importance: The higher the $\bar{M}_{w,\,Arm}$, the more sensitive it is to sonic degradation.

It is interesting to compare the sonic degradation behavior of linear PIB and *-(PIB)$_n$s. The linear PIB breaks into lower molecular weight fragments upon sonication: The eluogram shows a tail at low molecular weights even after 5 minutes of sonication, and the amount of this lower molecular weight fraction increases (multimodal) after 10–20 minutes. With continued sonication (after 40 minutes), the amount of the low molecular weight fragment increases and becomes the major product.

According to these studies, higher order stars are very sensitive to sonication. A small amount of higher order stars strongly increases the kinematic viscosity; however, sonication even for 5 minutes decreases the kinematic viscosity. The high sonic sensitivity of higher order stars is most likely due to the tight packing of numerous PIB arms enamating from a relatively small and compact PDVB core. In the presence of higher order stars, the degradation of primary stars and unlinked arms is delayed. Degradation increases with molecular weight of PIB arms.

CONCLUSIONS

Dilute solution viscosities of select monodisperse *-(PIB)$_n$s and linear PIBs in toluene over the 30 to 100°C range were investigated. The efflux times of solvent and stars decreased with increasing temperature. The intrinsic viscosities of stars are much lower than those of linear PIBs of the same molecular weight, and are close to those of "two-arm" stars and of the PIB arm. The $[\eta]_{Star}$ is mainly determined by the arm molecular weight and not by the total molecular weight of the star. While the $[\eta]_{Star}$ and the $[\eta]_{Linear}$ of the arm increase only slightly with temperature, the $[\eta]_{Linear}$ of high molecular weight linear PIB increases significantly with increasing temperature. The difference in the viscosity behavior of the stars and PIBs of the same molecular weight is due to the difference between their hydrodynamic volumes and mobilities. The g^*s of stars are small and decrease slightly with increasing temperature. A comparison between calculated and experimentally observed R_gs suggests that the structure of a star is much closer to the rigid sphere than to the random coil. The expansion of the ensemble of arms of the stars is severely restricted because the core-bonded chain ends are practically immobile. Short arms are expected to be essentially extended (rigid sphere limit) so that their temperature response will be insignificant. In contrast, long arms increasingly assume random coil-like conformations upon moving away from the congested core—toward the random coil limit because of the gradually increasing free volume. Transmission electron micrography of a star showed a sphere with a diameter of 55 ± 4 nm. This

size is in reasonably good agreement with $R_g = 27 \pm 2$ nm obtained by LLS. The viscosity indices of representative oil solutions of *-(PIB)$_n$s were in the 130 to 137 range and were moderately sensitive to the $\overline{M}_{w,\,Arm}$. The pour points of both *-(PIB)$_n$s and linear PIB oil solutions were -27°C, which is similar to that of a commercial polyisoprene star viscosity improver. Investigations of sonic shear stability of select *-(PIB)$_n$s and a linear PIB arm showed the kinematic viscosities of stars with short arms to level off after 20 minutes while the stars with long arms and linear PIB continued to lose viscosity. According to SEC analysis, higher order stars are very sensitive to sonication; however, the break-up of such stars decreases the kinematic viscosities after 5 minutes of sonication. The presence of higher order stars postpones the degradation of *-(PIB)$_n$s and unlinked arms. The molecular weight of the PIB arms is also important: High molecular weight increases the rate of degradation.

*-(PIB)$_n$s of optimum microarchitecture may become useful motor oil additives: Low molecular weight arms are resistant toward degradation but higher molecular weight arms are necessary to maintain a desirable kinematic viscosity for lubrication. The effect of the number of arms in this respect was not investigated. According to viscosity index, pour point, and sonic shear stability investigations, *-(PIB)$_n$s may be of importance as rheology improvers. Optimization of *-(PIB)$_n$ composition, including $\overline{M}_{w,\,Arm}$, $\overline{N}_{w,\,Arm}$, and core, would be fundamental to achieve this objective.

ACKNOWLEDGMENTS

This material is based upon work supported by the National Science Foundation under Grant DMR-9423202. The authors thank Prof. D. H. Napper (The University of Sydney) and Dr. L. J. Fetters (Exxon) for valuable discussions on dilute solution viscometry measurements, and Prof. D. H. Reneker and Dr. T. N. Georgiadis (The University of Akron) for help with electron microscopy. We thank Dr. M. J. Covitch (Lubrizol) for sonications and for his many comments and suggestions to improve the quality of our manuscript. Insightful discussions with Dr. F. Gruber (BASF) are gratefully acknowledged.

REFERENCES

[1] L.-K. Bi and L. J. Fetters, *Macromolecules, 9*, 732 (1976).
[2] I. Duvdevani, J. V. Fusco, K. W. Powers, and H.-C. Wang, Presentation at IRC-92, Beijing, People's Republic of China, 1992.
[3] H.-C. Wang, K. W. Powers, and J. V. Fusco, Lecture at Rubber Division, American Chemical Society, Mexico City, Mexico, 1989.
[4] P. F. Romeo, H.-C. Wang, and L. M. Wheeler, *Polym. Prepr., 31*(1), 460 (1990).
[5] P. F. Romeo, H.-C. Wang, and L. M. Wheeler, Lecture at Spring Meeting, American Chemical Society, Boston, MA, 1990.
[6] G. V. Strate and M. J. Struglinski, Lecture at Division of Polymeric Materials: Science and Engineering, American Chemical Society, Miami Beach, FL, 1989.

[7] M. A. Carignano and I. Szleifer, *Macromolecules, 27*, 702 (1994).
[8] D. Gersappe, P. K. Harm, D. Irvine, and A. C. Balazs, *Ibid., 27*, 720 (1994).
[9] J. T. Gotro and W. W. Graessley, *Ibid., 17*, 2767 (1984).
[10] S. Stinson, *Chem. Eng. News*, p. 7 (June 6, 1994).
[11] L. J. Fetters, A. D. Kiss, D. S. Pearson, G. F. Quack, and F. J. Vitus, *Macromolecules, 26*, 647 (1993).
[12] E. L. Thomas, D. B. Alward, D. J. Kinning, D. C. Martin, D. L. Handlin, and L. J. Fetters, *Ibid., 19*, 2197 (1986).
[13] P. R. Soskey, I. Duvdevani, H.-C. Wang, and T. E. Richards, Lecture at Rubber Division, American Chemical Society, Detroit, MI, 1989, Paper 54.
[14] L. Gruskey, J. V. Fusco, I. Duvdevani, and T. Takeda, *Ibid.*, Paper 55.
[15] G. V. Strate and M. J. Struglinski, *ACS Symp. Ser., 462*, Chap. 15 (1991).
[16] L. Gruskey, J. V. Fusco, I. Duvdevani, and T. Takeda, *Rubber World, 202*, 41 (1990).
[17] G. V. Strate and M. J. Struglinski, *Polym. Mater. Sci. Eng., 61*, 252 (1989).
[18] J. A. Simms and H. J. Spinelli, *J. Coatings Technol., 59*, 125 (1987).
[19] Shell Oil Co., Brochure 35 (1986).
[20] J. A. Simms, *Rubber Chem. Technol., 64*, 139 (1991).
[21] H. C. Kan, J. D. Ferry, and L. J. Fetters, *Macromolecules, 13*, 1571 (1980).
[22] I. Yamaoka and M. Kimura, *Polymer, 34*, 439 (1993).
[23] G. C. Meyer and J. M. Windmaier, *Polym. Eng. Sci., 17*, 803 (1977).
[24] J. P. Kennedy, T. M. Marsalkó, and I. Majoros, US Patent 5,395,885; World Patent 95/16727; *Chem. Abstr.*, 123, 56889x (1995).
[25] T. M. Marsalkó, I. Majoros, and J. P. Kennedy, *Polym. Bull., 31*(6), 665 (1993).
[26] T. M. Marsalkó, I. Majoros, and J. P. Kennedy, *Polym. Prepr., 35*(2), 504 (1994).
[27] T. M. Marsalkó, I. Majoros, and J. P. Kennedy, *Makromol. Chem., Macromol. Symp., 95*, 39 (1995).
[28] T. M. Marsalkó, I. Majoros, and J. P. Kennedy, *Polym. Mater. Sci. Eng., 73*, 181 (1995).
[29] T. M. Marsalkó, I. Majoros, and J. P. Kennedy, *Polym. Prepr., 37*(1), 581 (1996).
[30] J. P. Kennedy, T. M. Marsalkó, and I. Majoros, *Makromol. Chem., Macromol. Symp., 107*, 319 (1996).
[31] R. F. Storey and K. A. Shoemake, *Polym. Prepr., 35*(2), 578 (1994).
[32] R. F. Storey, K. A. Shoemake, and B. J. Chisholm, *J. Polym. Sci. Part A: Polym. Chem., 34*, 2003 (1996).
[33] DIN 53 012.
[34] B. J. Bauer and L. J. Fetters, Rubber Reviews for 1978, *Rubber Chem. Technol., 51*, 406 (1978).
[35] B. J. Bauer, N. Hadjichristidis, G. Quack, J. Vitus, and L. J. Fetters, *Polym. Prepr., 20*(2), 126 (1979).
[36] J. Roovers, L.-L. Zhou, P. M. Toporowski, M. V. D. Zwan, H. Iatrou, and N. Hadjichristidis, *Macromolecules, 26*, 4324 (1993).
[37] S. Bywater, *Adv. Polym. Sci., 30*, 89 (1979).
[38] J. J. Freire, A. Rey, M. Bishop, and J. H. R. Clarke, *Macromolecules, 24*, 6494 (1991).

[39] H. Benoit, J. F. Joanny, G. Hadzioannou, and B. Hammouda, *Ibid., 26*, 5790 (1993).
[40] S. F. Sun, S. Lin, and D. Sun, *Polym. Prepr., 25*(2), 71 (1984).
[41] F. Ganazzoli and A. Forni, *Macromolecules, 28*, 7950 (1995).
[42] A. Rey, J. J. Freire, M. Bishop, and J. H. R. Clarke, *Ibid., 25*, 1311 (1992).
[43] M. K. Mishra, *Macromol. Rep., A29*, vii (1992).
[44] S. F. Sun, D. K. Sun, and S. Liu, *Polymer, 26*, 1172 (1985).
[45] J. R. Schaefgen and P. J. Flory, *J. Am. Chem. Soc., 70*, 2709 (1948).
[46] S. F. Sun, *Polymer, 28*, 283 (1987).
[47] H. J. M. A. Mieras, *J. Polym. Sci., Polym. Symp., 42*, 987 (1973).
[48] J. Brandrup and E. H. Immergut, *Polymer Handbook*, 3rd ed., Wiley, New York, NY, 1991.
[49] W. H. Stockmayer and M. Fixman, *Ann. N. Y. Acad. Sci., 57*, 334 (1953).
[50] B. H. Zimm and R. W. Kilb, *J. Polym. Sci., 37*, 19 (1959).
[51] B. H. Zimm and W. H. Stockmayer, *J. Chem. Phys., 17*, 1301 (1949).
[52] D. H. Napper, The University of Sydney, Personal Communication, 1994.
[53] L. J. Fetters, Exxon, Personal Communication, 1995.
[54] A. Z. Ackasu and C. C. Han, *Macromolecules, 12*, 276 (1979).
[55] F. W. Billmeyer, *Textbook of Polymer Science*, Wiley, New York, NY, 1984.
[56] *ASM Materials Engineering Dictionary* (J. R. Davis, Ed.), Davis & Associates: ASM International, 1992.
[57] ASTM D 2270-91.
[58] ASTM D 97-87.
[59] W. J. Bartz, *Reiche Tribotechnik, Vol. 2*, C. R. Vincent Verlag, Hannover, 1992.
[60] D. B. Alward, D. J. Kinning, E. L. Thomas, and L. J. Fetters, *Macromolecules, 19*, 215 (1986).
[61] J. M. Warakomski, *Chem. Mater., 4*, 1000 (1992).
[62] M. T. Krejchi, Stanford University, Personal Communication, 1995.
[63] ASTM D 3945-86.
[64] ASTM D 5119-92.
[65] M. J. Covitch, The Lubrizol Corporation, Personal Communication, 1995.
[66] M. K. Mishra, Texaco R&D, Personal Communication, 1996.
[67] G. J. Price and P. F. Smith, *Eur. Polym. J., 29*, 419 (1993).
[68] ASTM D 2603-91.

Received August 10, 1996